Bias-dependent electrical spin generation in Fe_3Si/GaAs: Consistent behavior in nonlocal and local spin valves and in the three-terminal configuration

Yori Manzke, Jens Herfort, and Manfred Ramsteiner*
Paul-Drude-Institut für Festkörperelektronik, Hausvogteiplatz 5-7, 10117 Berlin, Germany
(Received 6 September 2017; published 26 December 2017)

We study spin generation in lateral spin-valve structures consisting of ferromagnetic Fe_3Si contacts on *n*-type GaAs transport channels. Different film-growth conditions are found to enable the comparison of ferromagnetic contacts with similar spin polarizations but different electrical characteristics. Strongly rectifying contacts are found to hinder the observation of spin-injection signals due to a strong bias dependence of the spin-generation efficiency. For contacts fabricated under optimized growth conditions, efficient spin generation enables the operation of nonlocal and local spin valves as well as the detection of spin signals in the three-terminal configuration. In all configurations, the observed signals exhibit a consistent bias-dependent spin generation and detection behavior which is explained by spin accumulation in the GaAs conduction band without the involvement of localized states.

DOI: 10.1103/PhysRevB.96.245308

I. INTRODUCTION

Many spintronic device concepts rely on an efficient electrical generation of a spin accumulation inside a semiconductor (SC) using the interface with a ferromagnetic metal (FM) [1]. Application of a reverse or forward bias voltage to an FM/*n*-type SC hybrid contact leads to the generation of spin-polarized electrons in the SC via spin injection or extraction, respectively [2]. Frequently used lateral transport structures include the nonlocal and the three-terminal (3T) geometries [3]. However, in systems utilizing oxide tunnel barriers, the results obtained in the 3T geometry are often found to be inconsistent with the expectations derived from the well-established detection of spin signals in the nonlocal spin-valve (NLSV) configuration [4–6]. For FM/insulator/*n*-Si tunnel junctions, for example, Tinkey *et al.* [5] recently claimed that the 3T magnetoresistance signal arises mostly from tunneling through impurities and defects in the interface proximity, rather than from spin accumulation due to elastic tunneling into the conduction band of the SC channel. On the other hand, for fully epitaxial systems with III-V SC channels and Schottky contacts forming the tunnel barrier, consistency between 3T and NLSV results has been reported (see, e.g., Nam *et al.* [7]). Regarding the technologically more relevant two-terminal arrangement of the local spin valve (LSV), reports on spin transport are scarce due to the difficulty to fulfill the specific requirements regarding the device parameters [8–10].

In our previous work we have established spin-transport structures consisting of Co_2FeSi contacts on *n*-type GaAs channels as a promising hybrid system for applications in the field of semiconductor spintronics [11]. The main motivation for choosing the Heusler alloy Co_2FeSi has been its complete spin polarization at the Fermi energy (half-metallic behavior). Indeed, with Co_2FeSi contacts the spin-generation efficiency could be improved by about one order of magnitude as compared to previously chosen ferromagnetic contacts in otherwise identical device structures [12–15]. For Co_2FeSi contact layers, we have further demonstrated the influence of the spin-polarized band structure on the spin transfer into *n*-type GaAs channels [16]. These studies benefited from the possibility to strongly modify the electronic band structure of Co_2FeSi by changing the film-growth conditions [17]. However, the leap in the spin-generation efficiency observed for Co_2FeSi contacts is most likely not only caused by the superior spin polarization. Even half-metallic behavior of the Co_2FeSi contacts could account only for a twofold improvement (considering a spin polarization of about 45% in the other FMs) [18–20]. In fact, one particular characteristic of Co_2FeSi contacts on *n*-type GaAs grown and investigated by our group is their relatively large leakage current under reverse bias conditions [11,16]. Consequently, it is natural to consider that an increased leakage current of the spin-injecting FM/SC contact could be beneficial for spin-generation experiments.

In this article we study the influence of the electrical contact characteristics on the spin-generation efficiency in lateral spin-transport structures with FM contact layers of similar spin polarization. For a FM/SC system with particularly advantageous electrical characteristics, we demonstrate spin generation in NLSV, LSV, and 3T configurations and find consistent results. Most significantly, our results obtained in the 3T configuration are in accordance with the spin-generation characteristics determined by NLSV measurements.

II. EXPERIMENTAL DETAILS

The investigated lateral spin-valve structures with *n*-type GaAs channels were grown by molecular beam epitaxy (MBE) on semi-insulating GaAs(001) substrates and processed by optical lithography [11]. Ferromagnetic contact layers consisting of Fe_3Si were chosen, since for this FM the spin polarization at the Fermi energy is expected to exhibit a relatively weak dependence on the growth conditions, in contrast to the full Heusler alloy Co_2FeSi [16]. The semiconductor layer sequence in all samples consists of a 1500-nm-thick, lightly *n*-type doped (5×10^{16} cm^{-3}) GaAs spin-transport layer followed by a 15-nm-thick layer with a linearly increasing doping density and a heavily doped (5×10^{18} cm^{-3}) 15-nm-thick layer leading to a narrow Schottky barrier which forms at the Fe_3Si/GaAs interface [14]. The 10-nm-thick Fe_3Si contact

*ramsteiner@pdi-berlin.de

 ©2017 American Physical Society

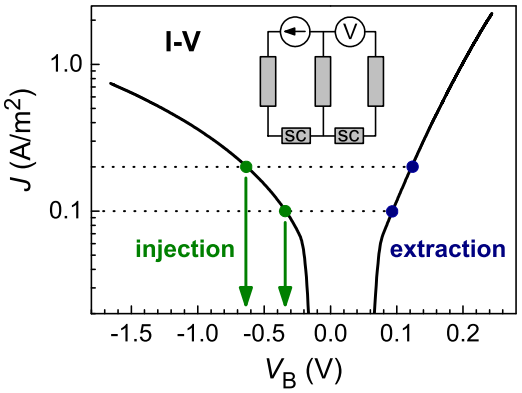

FIG. 1. Current-voltage (I-V) characteristic of a FM/SC contact measured in a three-terminal arrangement (see inset) with the current density given in absolute values. Bias voltages needed to obtain a charge current density in the range between 0.1 and 0.2 A/m^2 (typical magnitude needed to detect spin signals) are indicated for spin-injection (reverse bias) and extraction (forward bias) conditions. Note that the shown I-V characteristic constitutes the advantageous case of LT-Fe_3Si contacts (see discussion in the main text). For the more rectifying HT-Fe_3Si and Co_2Fe contacts (see Fig. 3), much higher bias voltages are needed to obtain the same current densities under injection (reverse bias) conditions.

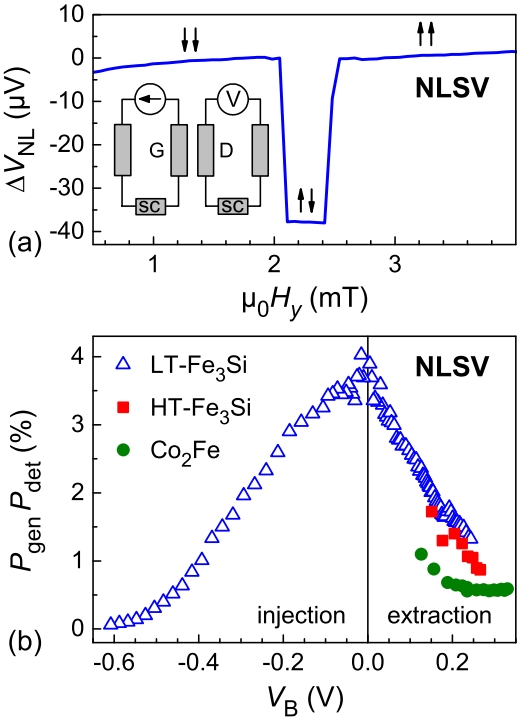

FIG. 2. (a) Typical spin-valve signal ΔV_{NL} obtained in the NLSV configuration (see inset) for $V_B = 0.15$ V (spin extraction) during an upward sweep of the external in-plane magnetic field (H_y) with a linear background signal subtracted (contacts G and D with strip widths of $W_G = 4\ \mu$m and $W_D = 5\ \mu$m, respectively, and a center-to-center separation of $d = 7.5\ \mu$m). (b) Effective spin-valve efficiency $P_{gen}P_{det}$ [see Eq. (1)] deduced for NLSV devices with LT-Fe_3Si ($W_G = 4\ \mu$m, $W_D = 5\ \mu$m, $d = 7.5\ \mu$m), HT-Fe_3Si ($W_G = 9\ \mu$m, $W_D = 22\ \mu$m, $d = 11.5\ \mu$m), and Co_2Fe ($W_G = 4\ \mu$m, $W_D = 5\ \mu$m, $d = 7.5\ \mu$m) contact layers as a function of the interface voltage V_B.

layers were deposited in a separate MBE growth chamber for metals at different substrate temperatures (50 and 200 °C). As evidenced by x-ray diffraction, the contact layer grown at high substrate temperature (HT-Fe_3Si) exhibits single crystalline ordering, whereas the one grown at low temperature (LT-Fe_3Si) is most likely polycrystalline or even amorphous. For reference purposes, an additional sample with contact layers consisting of the crystalline alloy Co_2Fe was prepared. The device structures comprise a $50 \times 400\ \mu$m^2 conductive mesa region with strip contacts and are described in more detail in Ref. [11]. For the present experiments, the center-to-center separations between the spin generation (injection or extraction) and detection contact strips were chosen to lie between 7.5 and 18.5 μm and the respective strip widths between 4 and 22 μm. All measurements were performed at 20 K in a He exchange gas cryostat, and electrical signals were recorded by a standard dc method. The experiments were conducted in the same manner as described, e.g., in Ref. [11].

III. RESULTS AND DISCUSSION

The current-voltage (I-V) characteristics of the FM/SC contacts have been measured in the three-terminal arrangement described, e.g., in Ref. [21]. Typical I-V characteristics, as shown in Fig. 1, exhibit a rectifying behavior, i.e., the absolute bias current as a function of the voltage drop at the FM/SC interface (V_B) is not symmetric with respect to the forward and reverse current directions. Under spin-injection conditions (reverse bias), the rectifying I-V characteristics result in relatively large interface voltages at significant bias currents. It is worth mentioning already here, that for a series of spin-valve structures investigated during recent years, spin-injection signals could only be observed for injector contacts showing an appreciable reverse current already at small bias voltage both in spin-LED [15] and NLSV measurements (with unbiased detector contacts) [11].

An example of successful spin generation and detection is illustrated in Fig. 2(a) for a lateral spin valve structure with LT-Fe_3Si contact strips. The nonlocal spin voltage measured in the NLSV configuration (see inset and Ref. [11]) for an unbiased spin-detecting contact is shown as a function of the external in-plane magnetic field. The observed voltage jump corresponds to the switching between parallel and antiparallel magnetization of the spin generating (G) and detecting (D) strips during an upward sweep of the magnetic field. This characteristic spin-valve signature provides clear evidence for the generation of spin-polarized electrons in the n-type GaAs channel. The sign of the observed voltage jumps is negative under spin-extraction conditions and found to be reversed under spin-injection conditions for the whole investigated range of bias voltages. This finding corresponds to majority-spin injection [22,25]. The spin transport between the spin-generating contact and the spin-detecting contact is assumed to be purely diffusive in our samples, because the spin-detecting contact is unbiased and the voltage probes are floating. According to the standard theory of spin injection, the nonlocal voltage signal ΔV_{NL} (normalized to the current density J) detected at a distance d from the point of spin

generation is given by [22,23]

$$\Delta V_{\mathrm{NL}}/J = P_{\mathrm{gen}} P_{\mathrm{det}} \lambda_{\mathrm{S}} \rho_{\mathrm{N}} \frac{W}{w} \exp(-d/\lambda_{\mathrm{S}}), \qquad (1)$$

with P_{gen} (P_{det}) denoting the effective spin-generation (detection) efficiency, λ_{S} is the spin diffusion length, W is the width of the spin generating contact, and ρ_{N} and w are the resistivity and thickness of the GaAs channel, respectively. A spin diffusion length of $\lambda_{\mathrm{S}} = 6.1 \pm 0.2$ μm has been determined from nonlocal spin-valve measurements using different contact spacings, which is in good agreement with previously reported values for n-type GaAs channels of similar doping level [9]. The other parameters can be inferred from conventional transport measurements (ρ_{N}) or are known geometrical factors according to the sample design (W and w).

The effective spin-valve efficiency $P_{\mathrm{gen}}P_{\mathrm{det}}$ extracted with Eq. (1) from the spin signals ΔV_{NL} obtained by NLSV measurements [see Fig. 2(a)] is shown in Fig. 2(b) as a function of the interface voltage V_{B} across the spin-generating contact (G). For both injection and extraction conditions, a pronounced decrease of the effective spin-valve efficiency with increasing absolute value of V_B is revealed. Bias dependencies of the spin-injection efficiency have been reported in the literature for spin-injection experiments both in the nonlocal and three-terminal geometries, including reports of a sublinear increase of the spin-induced nonlocal voltage with current or a decay of P_{gen} with increasing forward and reverse bias [22,24–28]. However, the reasons for the respective behaviors have not always been unambiguously identified.

The physical mechanisms that are potentially responsible for the decay of P_{gen} with bias can be grouped into processes which have an influence on the actual polarization of the tunneling current across the Schottky barrier on the one hand and spin relaxation mechanisms in the semiconductor on the other hand. Naturally, the spin polarization of the tunneling current depends on the spin-dependent band structure of the FM [16]. For a forward-biased contact, the bias dependence of the spin extraction efficiency is directly influenced by the energy dependence of the spin-dependent density of states above the Fermi level in the FM. In fact, a decay of the spin polarization in Fe_3Si with increasing energy can be found by comparing the calculated density of states for the two spin channels presented in Ref. [29]. Consequently, the influence of the band structure on the spin extraction process can be identified as the likely cause for the decay of the extraction efficiency with increasing forward bias. However, for reverse bias, the spin polarization at the Fermi energy should dominate the spin-injection process on the FM side. For large reverse bias voltages, electrons can tunnel from the ferromagnet into bands other than the Γ valley of GaAs, namely the L and X valleys, which exhibit short spin lifetimes [30,31]. As pointed out in Ref. [32], the spin-injection efficiency is consequently expected to decay for interface voltages beyond 300 mV. Furthermore, spin relaxation processes related to the electric field in the interface proximity region can lead to a bias dependent spin-injection efficiency [33]. In general, a decrease of the barrier resistance with increasing bias voltage may also lead to a decrease in the spin-injection efficiency because of the feedback of the spin accumulation on the spin current [4].

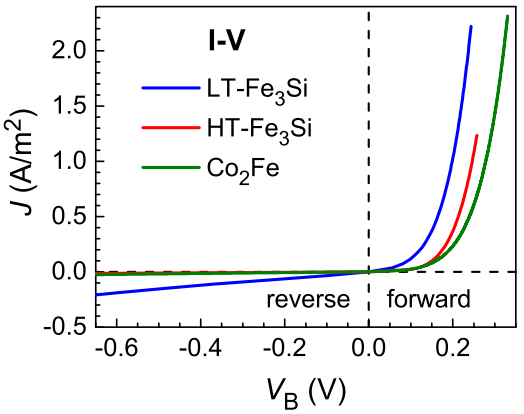

FIG. 3. Current-voltage (I-V) characteristics of FM/SC contacts containing LT-Fe_3Si, HT-Fe_3Si, and Co_2Fe contact layers measured in a three-terminal configuration.

However, the investigated contacts in this work are too resistive to be affected by the feedback problem.

Despite the strong bias dependence, successful spin generation and detection for both spin-injection and extraction conditions have been achieved in the case of LT-Fe_3Si contacts [see Fig. 2(b)]. For the FM/SC structures with HT-Fe_3Si and Co_2Fe contacts, in contrast, spin signals in the NLSV configuration could be detected only under spin extraction conditions. The absence of spin-injection signals for the FM/SC structures with HT-Fe_3Si and Co_2Fe contacts is caused by their strongly rectifying I-V characteristics (see Fig. 3) and the resulting large bias voltages needed to obtain a decent current density which is needed to detect spin signals [see, e.g., Eq. (1): $\Delta V_{\mathrm{NL}} \propto J$]. In the case of the LT-Fe_3Si contacts, in contrast, a significant current density under reverse bias conditions (cf. Fig. 3) enables the observation of spin signals induced by spin injection in the voltage range down to -0.6 V. The I-V characteristics shown in Fig. 3 were analyzed using the expressions given in Ref. [34] [Eqs. (14) and (40) for forward and reverse bias conditions, respectively]. However, for the present case of a heavily doped interlayer, the obtained diode parameters have to be regarded as rough estimates. Nevertheless, the fittings of the I-V curves indicate that the effective Schottky barrier height of the LT-Fe_3Si contact (0.25 eV) is reduced by about a factor of 2 with respect to the HT-Fe_3Si and Co_2Fe contacts (temperature-dependent ideality factors between 2 and 45 in each case, but constant tunneling parameters E_{00} as expected for pure field emission). A reduced Schottky barrier height is actually expected for uncompensated heavily doped (above 5×10^{17} cm^{-3}) GaAs. In this case, the localized states at the FM/SC interface can be assumed to be completely occupied due to the large concentration of electrically active Si donors. Consequently, the Fermi energy at the FM/SC interface is no longer pinned by the localized states but shifts towards the bottom of the conduction band [35]. Pronounced electrical compensation of the n-type doping is able to reverse this balance again. In this way, the Fermi level pinning depends on the interplay between the incorporation of Fe and Co as compensating deep acceptors and the formation of electrically inactive precipitates. Based on this consideration, a Schottky barrier

height around 0.25 eV (close to the separation between conduction band edge and the Fermi energy in degenerate n-type GaAs with a carrier density of 5×10^{18} cm^{-3}) would be in accordance with the intended, i.e., uncompensated, doping profile of our samples. The corresponding negligible degree of electrical compensation in the LT-Fe_3Si sample could obviously be enabled by the low substrate temperature used for the Fe_3Si growth. The larger Schottky barrier height of the HT-Fe_3Si contacts most likely originates from atomic exchange reactions at the FM/SC interface which are promoted by higher growth temperatures, especially for Fe containing FM films [36–38]. Selective exchange reactions, in particular, influence the GaAs stoichiometry at the interface proximity and, thus, the density of electronic gap states which are responsible for Fermi level pinning and the Schottky barrier formation [39,40]. Furthermore, the degree of electrical compensation resulting from the incorporation of Fe impurities and the temperature-dependent formation of Fe precipitates in the GaAs lattice might play an important role for the Fermi level pinning and the resulting Schottky barrier height [41–43]. All in all, our results demonstrate that the I-V characteristics of Fe_3Si/GaAs contacts can be adjusted to a certain degree by the MBE growth temperature. At the same time, the spin polarization at the Fermi energy in the conduction band of LT-Fe_3Si and HT-Fe_3Si contacts appears to be very similar as suggested by the coinciding effective spin-valve efficiency under spin extraction conditions [see Fig. 2(b)]. Consequently, the difference in the spin-generation properties of the two different Fe_3Si/SC contacts appears to mainly stem from their specific spin-independent electrical characteristics.

Utilizing the advantageous electrical characteristics of the LT-Fe_3Si contacts, we have been able to measure spin signals also in the LSV and the 3T configurations. Figure 4 displays the corresponding spin signals as a function of the external magnetic field. In analogy to the case of the NLSV measurement [see Fig. 2(a)], the magnetoresistance jump observed in the LSV configuration [cf. Fig. 4(a)] constitutes the characteristic spin-valve signature which provides evidence for electrical generation and detection of spin-polarized carriers in the GaAs channel. Remarkably, the detected LSV signal for low bias voltages corresponding to a magnetoresistance ratio of 0.016% is in exact agreement with the expectation for our device parameters [8]. For 3T measurements, the same ferromagnetic contact is used for the generation (G) and for the detection (D) of the electrically generated spin accumulation. The observed dependencies of the spin signal on both out-of-plane and in-plane magnetic fields [cf. Fig. 4(b)] reveal the commonly observed normal and inverted Hanle curves, respectively [4]. In contrast to the NLSV geometry, no spin-induced signals could be observed for the 3T geometry using spin-injection conditions. The reasons for this finding are twofold: First, the absolute signals are small for spin injection, because efficient spin injection is limited to the small forward bias region only [cf. Fig. 2(b)], and second, the large contact resistance of the reverse-biased Schottky contact leads to a large offset signal in the interface voltage. Therefore, the absolute voltage noise is substantially stronger in the negative voltage range, preventing the observation of Hanle curves. A spin lifetime τ_S of about 20 ns was extracted from the 3T Hanle curves using the expression given in Ref. [44].

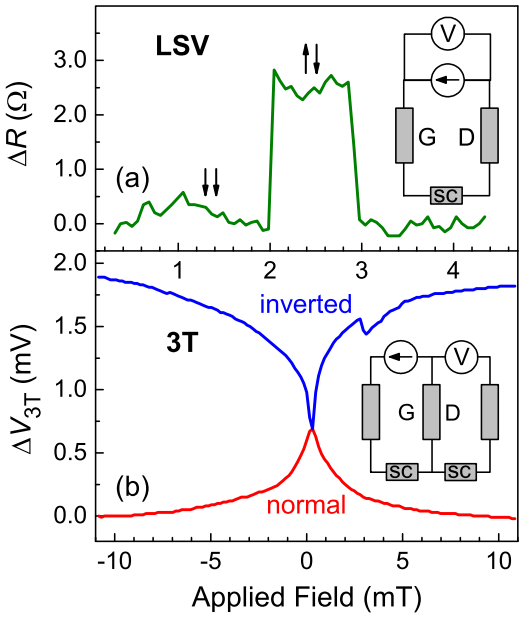

FIG. 4. (a) Magnetoresistance signal ΔR measured for a LSV device (see inset) with an LT-Fe_3Si contact layer during an upward sweep of the external in-plane magnetic field (contacts G and D with strip widths of 4 and 5 μm, respectively, and a center-to-center separation of 7.5 μm). A constant background resistance has been subtracted. (b) Corresponding spin-valve signal ΔV_{3T} obtained in the three-terminal (3T) configuration (see inset) under spin-extraction conditions ($V_B = 0.18$ V) during sweeps of external out-of-plane (normal Hanle curve) and in-plane (inverted Hanle curve) magnetic fields (outer contacts and inner contact with strip widths of 4 and 5 μm, respectively, and center-to-center separations of 7.5 μm). A constant background voltage has been subtracted. The small feature in the inverted Hanle curve at 3 mT originates most likely from a magnetization switching.

Furthermore, a spin lifetime of 28 ns was estimated from NLSV Hanle measurements (not shown) from the expression given in Ref. [11] and using the relation $\lambda_S = \sqrt{D\tau_S}$ for the spin diffusion constant D. Both values agree reasonably well given possible distortions, e.g., due to dynamic nuclear polarization [45]. Furthermore, the magnitude of the 3T signal agrees well with the NLSV signal extrapolated for $d = 0$. These results indicate that the 3T signals observed in the LT-Fe_3Si sample are indeed caused by a spin accumulation in the SC channel. For various other FM/SC material systems, in contrast, a lack of consistency between the spin lifetimes obtained by NLSV and 3T measurements has been reported [6].

For a further confirmation that spin accumulation is the origin of the presently reported 3T signals, we compare the bias dependencies of the 3T and NLSV signals. Whereas the NLSV signal is proportional to $P_{gen}P_{det}$ [see Eq. (1)], the spin signal in the 3T configuration is proportional to P_G^2, the square of the tunnel spin polarization [4]. P_G can be deduced from the 3T measurements and is expected to correspond to P_{gen} obtained from the NLSV signals. The detection efficiency P_{det} is related to the unbiased detecting contact in the nonlocal configuration and is thus independent of V_B. With the approximation $P_{det} = P_{gen}$ at low bias voltages, we are able to deduce the 3T efficiency product $P_G P_{det}$ which is shown together with the

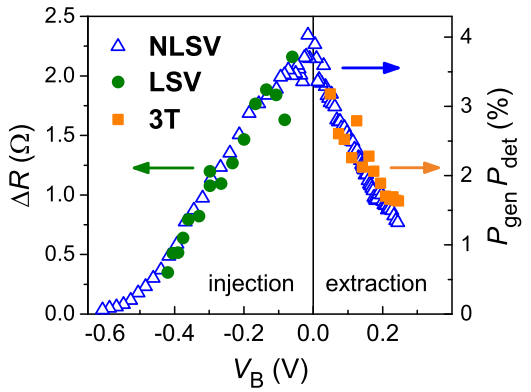

FIG. 5. Bias dependencies of the NLSV efficiency product $P_{gen}P_{det}$ [see Eq. (1)] and the 3T efficiency product $P_G P_{det}$ (see text) for devices with LT-Fe_3Si contacts. The corresponding 3T signal is given by the difference between the inverted and normal Hanle voltages measured at 10 mT [see Fig. 4(b)]. In addition, the corresponding magnetoresistance signal ΔR measured in the LSV configuration is shown as a function of the interface voltage V_B. For all configurations, contacts with strip widths of 4 to 5 μm and center-to-center separations of 7.5 μm were used (cf. Figs. 2 and 4).

NLSV efficiency product $P_{gen}P_{det}$ in Fig. 5 as a function of V_B. The good agreement between the bias dependencies of the two efficiency products confirms the common origin of the 3T and NLSV signals. For the NLSV operation, spin transport via itinerant electrons between the generating and the detecting contacts is required so that a spin accumulation in localized states is not relevant. Consequently, direct spin accumulation in the GaAs conduction band is found to be the underlying spin-generation mechanism responsible for both the NLSV and 3T signals with the effective spin-generation efficiency P_{gen} being approximately equal to the tunnel spin polarization P_G. In contrast to spin-valve structures with oxide barriers and group IV transport channels, spin-related processes in the interface proximity region appear to be of minor importance for the present MBE grown hybrid system with a group III-V transport channel. For another fully epitaxial FM/SC system without oxide barrier, Nam *et al.* [7] arrive at the same conclusion.

Finally, the operation of the LSV is expected to be limited by the bias dependence of the spin-injection efficiency. The LSV spin signal corresponds to the measured voltage between the reverse-biased ferromagnetic spin-injecting contact and a second forward-biased contact. Because the voltage drop across the forward-biased contact is negligible, the bias dependence of the measured LSV spin signal is dominated by that of spin-injecting contact. Indeed, as shown in Fig. 5, the bias dependence of the LSV signal is seen to track the decay of the NLSV signal for spin-injection conditions, which indicates that both types of spin valves are limited by the same V_B dependent mechanism. Altogether, the comparison of the different spin-valve geometries for a single device provides direct evidence for a common origin of the spin signals: Spin accumulation in the conduction band of GaAs and not from localized states. For this result, the reduced reactivity at the FM/SC interface at low growth temperatures is again of benefit, in addition to the formation of contacts with advantageous electrical characteristics.

IV. SUMMARY AND CONCLUSIONS

The strong bias dependence of the spin-generation efficiency imposes severe requirements on the electrical characteristics of ferromagnetic contacts on GaAs channels. In particular, the observation of spin injection is hindered by strongly rectifying contacts. For Fe_3Si/GaAs contacts, the I-V characteristics can be improved to a certain degree by adjusting the film-growth conditions. For optimized contacts, a consistent lateral spin-transport behavior is found for the nonlocal and local spin-valve configurations as well as the three-terminal configuration. For the present hybrid system without an oxide barrier, the three-terminal signal truly stems from a direct spin generation in the GaAs conduction band rather than from a spin accumulation in localized states.

ACKNOWLEDGMENTS

We acknowledge the expert technical support by W. Anders, A. Riedel, and G. Paris as well as the critical reading of the manuscript by O. Brandt.

[1] I. Žutić and S. Das Sarma, Rev. Mod. Phys. **76**, 323 (2004).
[2] A. M. Bratkovsky, Rep. Prog. Phys. **71**, 026502 (2008).
[3] J. Shiogai, M. Ciorga, M. Utz, D. Schuh, M. Kohda, D. Bougeard, T. Nojima, J. Nitta, and D. Weiss, Phys. Rev. B **89**, 081307 (2014).
[4] R. Jansen, S. P. Dash, S. Sharma, and B. C. Min, Semicond. Sci. Technol. **27**, 083001 (2012).
[5] H. N. Tinkey, P. Li, and I. Appelbaum, Appl. Phys. Lett. **104**, 232410 (2014).
[6] O. Txoperena and F. Casanova, J. Phys. D. Appl. Phys. **49**, 133001 (2016).
[7] S. H. Nam, T.-E. Park, Y. H. Park, H.-I. Ihm, H. C. Koo, H.-J. Kim, S. H. Han, and J. Chang, Appl. Phys. Lett. **109**, 122409 (2016).
[8] A. Fert, J.-M. George, H. Jaffres, and R. Mattana, IEEE Trans. Electron Devices **54**, 921 (2007).
[9] M. Ciorga, C. Wolf, A. Einwanger, M. Utz, D. Schuh, and D. Weiss, AIP Adv. **1**, 022113 (2011).
[10] T. Sasaki, T. Suzuki, Y. Ando, H. Koike, T. Oikawa, Y. Suzuki, and M. Shiraishi, Appl. Phys. Lett. **104**, 052404 (2014).
[11] P. Bruski, Y. Manzke, R. Farshchi, O. Brandt, J. Herfort, and M. Ramsteiner, Appl. Phys. Lett. **103**, 052406 (2013).
[12] H. J. Zhu, M. Ramsteiner, H. Kostial, M. Wassermeier, H.-P. Schönherr, and K. H. Ploog, Phys. Rev. Lett. **87**, 016601 (2001).
[13] M. Ramsteiner, H. Y. Hao, A. Kawaharazuka, H. J. Zhu, M. Kästner, R. Hey, L. Däweritz, H. T. Grahn, and K. H. Ploog, Phys. Rev. B **66**, 081304 (2002).

[14] A. Kawaharazuka, M. Ramsteiner, J. Herfort, H.-P. Schönherr, H. Kostial, and K. H. Ploog, Appl. Phys. Lett. **85**, 3492 (2004).
[15] M. Ramsteiner, O. Brandt, T. Flissikowski, H. T. Grahn, M. Hashimoto, J. Herfort, and H. Kostial, Phys. Rev. B **78**, 121303(R) (2008).
[16] P. Bruski, S. C. Erwin, J. Herfort, A. Tahraoui, and M. Ramsteiner, Phys. Rev. B **90**, 245150 (2014).
[17] M. Hashimoto, A. Trampert, J. Herfort, and K. H. Ploog, J. Vac. Sci. Technol. B **25**, 1453 (2007).
[18] R. J. Soulen, Jr., J. M. Byers, M. S. Osofsky, B. Nadgorny, T. Ambrose, S. F. Cheng, P. R. Broussard, C. T. Tanaka, J. Nowak, J. S. Moodera, A. Barry, and J. M. D. Coey, Science **282**, 85 (1998).
[19] R. P. Panguluri, G. Tsoi, B. Nadgorny, S. H. Chun, N. Samarth, and I. I. Mazin, Phys. Rev. B **68**, 201307 (2003).
[20] A. Ionescu, C. A. F. Vaz, T. Trypiniotis, C. M. Gürtler, H. García-Miquel, J. A. C. Bland, M. E. Vickers, R. M. Dalgliesh, S. Langridge, Y. Bugoslavsky, Y. Miyoshi, L. F. Cohen, and K. R. A. Ziebeck, Phys. Rev. B **71**, 094401 (2005).
[21] T. Uemura, K. Kondo, J. Fujisawa, K.-i. Matsuda, and M. Yamamoto, Appl. Phys. Lett. **101**, 132411 (2012).
[22] M. Ciorga, A. Einwanger, U. Wurstbauer, D. Schuh, W. Wegscheider, and D. Weiss, Phys. Rev. B **79**, 165321 (2009).
[23] T. A. Peterson, S. J. Patel, C. C. Geppert, K. D. Christie, A. Rath, D. Pennachio, M. E. Flatté, P. M. Voyles, C. J. Palmstrøm, and P. A. Crowell, Phys. Rev. B **94**, 235309 (2016).
[24] Y. Ando, K. Kasahara, K. Yamane, Y. Baba, Y. Maeda, Y. Hoshi, K. Sawano, M. Miyao, and K. Hamaya, Appl. Phys. Lett. **99**, 012113 (2011).
[25] Q. O. Hu, E. S. Garlid, P. A. Crowell, and C. J. Palmstrøm, Phys. Rev. B **84**, 085306 (2011).
[26] K.-R. Jeon, B.-C. Min, I.-J. Shin, C.-Y. Park, H.-S. Lee, Y.-H. Jo, and S.-C. Shin, Appl. Phys. Lett. **98**, 262102 (2011).
[27] T. Uemura, T. Akiho, M. Harada, K.-i. Matsuda, and M. Yamamoto, Appl. Phys. Lett. **99**, 082108 (2011).
[28] A. Dankert, R. S. Dulal, and S. P. Dash, Sci. Rep. **3**, 3196 (2013).
[29] B. Hamad, J. Khalifeh, I. A. Aljarayesh, C. Demangeat, H.-B. Luo, and Q.-M. Hu, J. Appl. Phys. **107**, 093911 (2010).
[30] S. Saikin, M. Shen, and M.-C. Cheng, J. Phys. Condens. Matter **18**, 1535 (2006).
[31] Y. Song and H. Dery, Phys. Rev. B **81**, 045321 (2010).
[32] G. Salis, S. F. Alvarado, and A. Fuhrer, Phys. Rev. B **84**, 041307 (2011).
[33] O. M. J. van 't Erve, A. L. Friedman, E. Cobas, C. H. Li, J. T. Robinson, and B. T. Jonker, Nat. Nanotechnol. **7**, 737 (2012).
[34] F. A. Padovani and R. Stratton, Solid State Electron. **9**, 695 (1966).
[35] V. Filipavičius, R. Gaidys, V.-A. Matulaitis, G. Petrauskas, A. Sakalas, and S. Sakalauskas, Phys. Status Solidi **99**, 543 (1987).
[36] L. J. Brillson, R. E. Viturro, C. Mailhiot, J. L. Shaw, N. Tache, J. McKinley, G. Margaritondo, J. Woodall, P. D. Kirchner, G. D. Pettit, and S. L. Wright, J. Vac. Sci. Technol. B **6**, 1263 (1988).
[37] C. Adelmann, J. Q. Xie, C. J. Palmstrøm, J. Strand, X. Lou, J. Wang, and P. A. Crowell, J. Vac. Sci. Technol. B **23**, 1747 (2005).
[38] L. R. Fleet, K. Yoshida, H. Kobayashi, Y. Ohno, H. Kurebayashi, J.-Y. Kim, C. H. W. Barnes, and A. Hirohata, IEEE Trans. Magn. **46**, 1737 (2010).
[39] R. van de Walle, R. L. Van Meirhaeghe, W. H. Laflère, and F. Cardon, J. Appl. Phys. **74**, 1885 (1993).
[40] C. S. Gworek, P. Phatak, B. T. Jonker, E. R. Weber, and N. Newman, Phys. Rev. B **64**, 045322 (2001).
[41] D. T. McInturff, E. S. Harmon, J. C. P. Chang, T. M. Pekarek, and J. M. Woodall, Appl. Phys. Lett. **69**, 1885 (1996).
[42] S. Hirose, M. Yamaura, S. Haneda, K. Hara, and H. Munekata, Thin Solid Films **371**, 272 (2000).
[43] R. Moriya, Y. Katsumata, Y. Takatani, S. Haneda, T. Kondo, and H. Munekata, Physica E **10**, 224 (2001).
[44] S. P. Dash, S. Sharma, R. S. Patel, M. P. de Jong, and R. Jansen, Nature (London) **462**, 491 (2009).
[45] C. Awo-Affouda, O. M. J. van 't Erve, G. Kioseoglou, A. T. Hanbicki, M. Holub, C. H. Li, and B. T. Jonker, Appl. Phys. Lett. **94**, 102511 (2009).